

Exchange narrowing of the J band of molecular dye aggregates

P. B. Walczak, A. Eisfeld,^{a)} and J. S. Briggs

Theoretische Quantendynamik, Universität Freiburg, Hermann-Herder-Str. 3, D-79104 Freiburg, Germany

(Received 24 September 2007; accepted 19 November 2007; published online 28 January 2008)

The exchange narrowing of the J band of certain dye monomers upon aggregation in solution has been known since the 1930s. Here, we analyze the theoretical explanations put forward to account for these narrow absorption bands. Although the theories range from models of identical monomers interacting with vibrations to the opposite of rigid monomers with statistically distributed electronic site energies, all approaches exhibit exchange narrowing. However, we show that the origins of the narrowing are different. A unified theory incorporating the two approaches is presented in which features of both narrowing mechanisms are evident. © 2008 American Institute of Physics.

[DOI: 10.1063/1.2823730]

I. INTRODUCTION

The changes in shape of the absorption spectrum of molecules when they aggregate provide clues as to the conformation of the aggregate and the strength and nature of the interaction between the monomers. Amongst the most striking of such spectral changes is the extreme redshift and narrowing of the broad vibronic absorption spectrum of a class of cyanine dyes subject to strong monomer-monomer coupling. The narrow shifted aggregate spectral line is known as the J band and occurs in many aggregates of dye molecules. Since its discovery in 1936,¹⁻³ the narrowing of the J band, nowadays called exchange narrowing, has been the subject of many theories. Here, it is perhaps appropriate to give a brief history of the development of our understanding of exchange narrowing.

Although Scheibe⁴ and Franck and Teller⁵ in 1938 correctly ascribed the J band as due to absorption to a collective state of electronic excitation, a Frenkel exciton, they advanced no explanation of its vibrational narrowing. The exciton interacts with vibrations in three ways. First, there is the dominant mode of intramolecular vibration accompanying electronic excitation which gives rise to a vibrational progression in the monomer spectrum. We will call this vibration intramolecular type 1 (IM1). Second, as high resolution data on cold monomers show⁶ that the dominant mode interacts with many “soft modes” of internal vibration, which contribute to an effective broadening of the vibrational progression. We will call these modes intramolecular type 2 (IM2), although noting that in specific monomers the distinction between IM1 and IM2 may be blurred and there may be more than one IM1 type of vibration. Third, there is the interaction of the vibrating monomer with the enormous number of soft modes of the surrounding solvent or matrix. This contributes greatly to the broadening of the monomer vibronic absorption bands at room temperatures. These external modes of vibration will be called EM. Both the interaction with IM2 and with EM can lead to transitions (relaxation) between levels of the dominant mode, or modes, IM1.

The question to be answered is: when the monomer absorption band is broadened into a quasi-continuum by these vibrational interactions, why does the J band exhibit a much-reduced broadening? We enumerate several approaches to answer this question.

- (i) In 1957, Simpson and Peterson⁷ (to be referred to as SP) advanced a qualitative argument based on the magnitude of a parameter (the SP parameter), which is the ratio of the purely electronic intermonomer interaction energy (which is $2V$ for linear aggregates and nearest-neighbor interaction V) compared to the vibrational width Δ of the monomer absorption band. The vibrational width Δ is usually of the order of a few $\hbar\omega$, where ω is the vibrational frequency on the upper potential curve. SP associated the strong-coupling case, when the aggregate shows a J band much narrower than the monomer band, with the case $2V/\Delta \gg 1$. This explanation of the narrowing is best understood in the time picture, where the strong-coupling condition in the aggregate implies that the electronic transfer time $\hbar/2V$ is much less than the vibrational relaxation time, which is the order of \hbar/Δ . There the vibrational wave packet, placed on the upper potential curve by a vertical Franck-Condon transition from the ground vibrational state, has no time to form standing vibrational waves before electronic excitation is passed on to the neighboring monomer. Then, as SP remark “the nuclear configuration is close to that for the ground state,” and the aggregate absorption spectrum should become infinitely narrow for an infinite chain with infinitely strong coupling. Based on this qualitative argument, SP presented a sketch (Fig. 2 in Ref. 7) showing the expected narrowing of the J band in strong coupling.
- (ii) Subsequently, in 1971, Briggs and Herzenberg⁸ showed that the ideas of SP are borne out by the first J -band theory, the coherent exciton scattering (CES) approximation, in which a continuous monomer vibronic spectrum was modeled. One can show that a single Gaussian peak for the monomer absorption is

^{a)}Electronic mail: alexander.eisfeld@physik.uni-freiburg.de.

- obtained when the upper potential curve is represented as a linear function. Then, there are no standing waves for the excited-state vibrational motion but only outgoing waves, corresponding to vibrational dissipation of IM1 energy into IM2 and solvent EM. The slope of the upper curve decides the width Δ of the Gaussian monomer spectrum and is proportional to the relaxation time. Hence, the SP criterion appears naturally. With a Gaussian monomer band, the aggregate spectrum can be calculated analytically. In particular, one can show⁸ that, in strong coupling, the width of the J band decreases exponentially with an exponent which is the square of the SP parameter, i.e., there is a strong narrowing as the coupling strength increases. Using a measured monomer spectrum, rather than the Gaussian model, it was shown^{9–12} that good agreement with the width of the J -band spectrum of several dye aggregates can be obtained. In Ref. 13, it has been shown analytically that, within the CES approximation, the precise width and shape of the J band depend crucially on the energy dependence of the *monomer* band-tail absorption. For later considerations, it should be noted that the CES result is independent of the number N of aggregated monomers.
- (iii) In two papers in 1977 and 1978, Klafter and Jortner^{14,15} considered the line shape of exciton absorption in molecular crystals but, as they assumed a one-dimensional model, the results are equally applicable to one-dimensional aggregates. The continuous line shape was attributed to two separate but related effects. The first is the assumption that each monomer has its electronic transition energy changed by interaction with the local environment. This coupling enters phenomenologically as a “diagonal disorder” or “static disorder” in the aggregate Hamiltonian. An effective continuous vibronic spectrum is obtained by assuming that electronic transition energies are distributed continuously according to an assumed Gaussian distribution, whose width is a free parameter. The second effect is the coupling of the purely electronic exciton to EM of the surroundings leading to “off-diagonal disorder.” Klafter and Jortner showed, using a Green’s function approach similar to that of the CES approximation, that both exciton-disorder and exciton-phonon scattering can be represented as separate contributions to a complex exciton self-energy. In a simultaneous paper,¹⁶ they applied the theory to derive absorption band tails of exponential Urbach form, although they had to make several assumptions about the exciton-phonon scattering. However, they did not specifically address the question of narrowing of the exciton band, although essentially they were considering the J -band absorption.
- (iv) Also, in 1977, Lukashin and Frank-Kamenetskii¹⁷ in a paper devoted primarily to dimer spectra suggested, without proof, that the J band will be narrowed by a factor of $1/\sqrt{N}$ compared to the monomer bandwidth. This conjecture was based on the known result¹⁸ that the dimer spectrum in strong coupling has a width of $1/\sqrt{2}$ smaller than that of the monomer.
- (v) In a 1984 paper,¹⁹ Knapp considered specifically the J -band narrowing and used the description “exchange narrowing” for this effect. In this approach, a purely electronic Hamiltonian is assumed, i.e., IM1 vibrations are ignored and IM2 and EM vibrations are not included explicitly. As in Klafter and Jortner, it was assumed that there is (static) diagonal disorder due to shifts of electronic transition energy at each monomer site. Knapp derived the analytic result that, when there is no intersite correlation between energy shifts, the aggregate linewidth in strong coupling diminishes according to $1/\sqrt{N}$. Note that in this result, the linewidth is independent of the SP parameter (with the width of the assumed Gaussian distribution as Δ), so long as it is large enough to ensure that the diagonal disorder is a perturbation on the electronic Hamiltonian. Also, this result is in line with the conjecture in Ref. 17. Knapp then went on to show that when the site energy shifts are correlated, the linewidth depends strongly on this degree of correlation. In particular, for infinitely strong correlation, the aggregate linewidth is unchanged from that of the monomer. The $1/\sqrt{N}$ narrowing was interpreted as due to averaging the inhomogeneities over all sites in the aggregate. However, he also recognized a basic problem with this result, namely, that the number N giving the width of the J band should not correspond to the number of aggregated monomers but rather to the number N_{coh} of monomers on the chain which are coherently coupled electronically, i.e., on the “size” of the exciton. The problem is how does one decide what is N_{coh} . Of course, if one believes the theory, one can work back from the measured spectrum to infer N_{coh} .
- (vi) In a further paper by Knapp *et al.* in 1984,²⁰ a rather different strategy was employed, in that phonons were included specifically. However, diagonal disorder was ignored in the aggregate Hamiltonian, which allowed the aggregate vibronic “stick” spectrum to be calculated by diagonalization of the Hamiltonian. Then, assuming a Gaussian shape instead of the monomer stick peaks, a modified form of the CES approximation was applied, resulting in a continuous aggregate spectrum and, in particular, a narrow J band in agreement with experiment. Although the origin of the narrowing of the J band can be explained analytically in CES approximation [see (ii) above], the authors attributed the narrowing to the exchange narrowing described by Knapp,¹⁹ even though diagonal disorder was ignored.
- (vii) In the following years, much effort was spent on investigating the influence of (diagonal and off diagonal) disorder on the spectral properties of aggregates.^{21–25} In 1990, Tilgner *et al.*²⁶ included both diagonal and off-diagonal static disorders in the purely electronic Hamiltonian and, following Knapp, they calculated a continuous aggregate spectrum by assuming Gaussian statistical distributions for the

monomer transition energies and nearest-neighbor couplings. In contrast, in 1991, in Ref. 22, the off-diagonal disorder was introduced through a Gaussian distribution of molecular positions. The numerical results showed that in this case, the narrowing was quite different from the case considered by Tilgner *et al.* This behavior was explained by Malyshev and Dominguez-Adame.²⁷ They showed that fluctuations in the positions lead to correlations in the interactions between the monomers. The extensive numerical calculations performed by Fidler *et al.*²² with an arbitrary degree of correlation between the random transition frequencies of the monomers confirmed Knapp's 1984 results. Within this approach, also good agreement between measured *J*-band spectra and theory has been obtained.²⁸

- (viii) In 1996, Scherer²⁹ considered an exciton interacting with both high-frequency IM1 and low-frequency IM2 (or EM) modes. Examples of aggregate spectra for two cases were given. First, for an exciton interacting with a single IM1 mode, stick spectra were presented for $N=8$ and various coupling strengths, illustrating the *J*-band narrowing for strong coupling. Second, a single IM1 mode was considered, together with a Gaussian distribution of diagonal energies leading to continuously broadened spectra, but only the example of intermediate coupling for $N=2$ to $N=8$ was presented.
- (ix) The problem of which N_{coh} is appropriate to estimate the *J* band width in purely electronic theories was addressed by Malyshev^{30,31} and Malyshev and Dominguez-Adame,²⁷ who gave a formula with which N_{coh} can be estimated. The basic result Malyshev derived is that in the case of diagonal disorder, one can estimate $N_{\text{coh}} \approx 1.5\pi^2|2V|/\Delta$ for a linear aggregate, thus directly connecting the delocalization length to the SP parameter.

This plethora of different theories underlies the difficulty of understanding precisely the origins of the *J*-band width. This paper attempts to shed some light on the problem by analyzing two theoretical approaches in more detail. First, we show (Sec. III) that, in a theory including only IM1 explicitly (i.e., working with vibronic stick spectra) and assuming identical monomers, one obtains also a predicted $1/\sqrt{N}$ narrowing of the *J*-band spectrum in the limit of strong coupling. This confirms the supposition mentioned in point (iv) above. The analytic result is a generalization of a result known for a long time for dimers, namely, that in strong coupling the spectrum has a width of $1/\sqrt{2}$ that of the monomer.^{18,32-34}

Second, we show (Sec. IV) that in purely statistical theories, ignoring vibrations altogether, the $1/\sqrt{N}$ narrowing arises quite generally without any specific assumptions as to the character of the statistical distribution, provided the variance exists. In this way, we identify the precise origin of the $1/\sqrt{N}$ narrowing in this case. Finally, we analyze in Sec. V

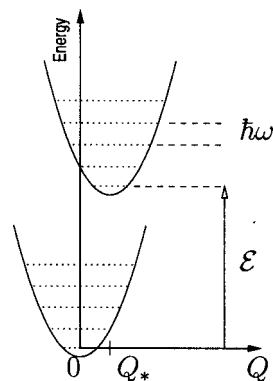


FIG. 1. Sketch of the BO potentials of the monomers.

the case in which both vibronic intramonomer coupling and a statistical spread of transition energies are taken into account.

II. THE BASIC HAMILTONIAN

First, we consider a monomer with a ground and only one excited electronic state and include intramonomer vibrations explicitly. In the Born-Oppenheimer (BO) approximation, the nuclei move on the ground- or excited-state potential energy surfaces (PESs) which are sketched in Fig. 1 for a single vibrational degree of freedom Q . We specialize to the particular approximation of harmonic vibrations of the same frequency in the upper and lower PESs, since it allows a simple analytic form [e.g., Eq. (17)] to be given for vibronic spectra. It also makes contact with previous work where the same approximation was used.^{18,32-37} Specifically, the energy difference between the minima of the PES is denoted by \mathcal{E} , the shift of the upper curve minimum by Q_* , and $\hbar\omega$ is the vibrational quantum. In the single-channel BO approximation, the wave functions in the electronic ground state are

$$|\Phi^g\rangle = |\phi^g\rangle|\chi^\alpha\rangle, \quad (1)$$

where $|\phi^g\rangle$ is the electronic part, parametrically dependent on Q , and $|\chi^\alpha\rangle$ denotes the α th vibrational wave function in the ground-state PES. Then, $|\chi^\alpha\rangle$ satisfies the equation

$$H^g|\chi^\alpha\rangle = \alpha\hbar\omega|\chi^\alpha\rangle, \quad (2)$$

where

$$H^g = \frac{1}{2}(P^2 + \omega^2Q^2) \quad (3)$$

is the vibrational Hamiltonian in the electronic ground state. Similarly, an excited-state vector of the monomer is written as

$$|\Phi^e\rangle = |\phi^e\rangle|\xi^\beta\rangle, \quad (4)$$

where $|\phi^e\rangle$ is the electronic part and $|\xi^\beta\rangle$ satisfies

$$H^e|\xi^\beta\rangle = (\beta\hbar\omega + \mathcal{E})|\xi^\beta\rangle, \quad (5)$$

with

$$H^e = \frac{1}{2}(P^2 + \omega^2(Q - Q_*)^2) + \mathcal{E}. \quad (6)$$

Within the electronic two-state approximation, the total monomer Hamiltonian is given by

$$\mathcal{H} \equiv \mathcal{H}^g + \mathcal{H}^e = H^g |\phi^g\rangle\langle\phi^g| + H^e |\phi^e\rangle\langle\phi^e|. \quad (7)$$

In an aggregate consisting of N monomers, we will label quantities belonging to the n th monomer with a subscript n .

The aggregate electronic ground-state vector $|g\rangle$ is taken as a simple product of the $|\phi_m^g\rangle$ of each monomer m , i.e.,

$$|g\rangle = \prod_{m=1}^N |\phi_m^g\rangle \quad (8)$$

for an aggregate comprised of N monomers. Similarly, the excited-state vectors of the aggregate are taken as localized vectors $|\pi_n\rangle$ denoting the n th monomer electronically excited and all others in the ground state, i.e.,

$$|\pi_n\rangle = |\phi_n^e\rangle \prod_{j \neq n} |\phi_j^g\rangle. \quad (9)$$

Then, generalizing Eq. (7) for the aggregate, one has

$$\mathcal{H}^g = \left(\sum_{n=1}^N H_n^g \right) |g\rangle\langle g| \quad (10)$$

in the electronic ground state and

$$\mathcal{H}^e = \sum_{n=1}^N \left(H_n^e + \sum_{m \neq n} H_m^g \right) |\pi_n\rangle\langle\pi_n| + \sum_{nm} V_{nm} |\pi_n\rangle\langle\pi_m| \quad (11)$$

for the electronic excited state of the aggregate. Here, the exchange matrix element V_{nm} , causing electronic excitation to be transferred from monomer n to monomer m via electron-electron interactions, is taken to be independent of nuclear coordinates. To obtain simple analytic formulas, we will assume that the vibrational frequency ω and the shift of the upper PES Q_* are independent of the monomer index n . Taking this into account and inserting the Hamiltonians of the monomers [Eqs. (3) and (6)] into Eq. (11), we obtain explicitly

$$\mathcal{H}^e = \sum_{n=1}^N \left(\frac{1}{2} (P_n^2 + \omega^2 (Q_n - Q_*)^2) + \mathcal{E}_n + \sum_{m \neq n} \frac{1}{2} (P_m^2 + \omega^2 Q_m^2) \right) \times |\pi_n\rangle\langle\pi_n| + \sum_{nm} V_{nm} |\pi_n\rangle\langle\pi_m|. \quad (12)$$

Note that the electronic transition energy \mathcal{E}_n is dependent on the monomer index n to account for diagonal disorder.

In the following section, we will first consider absorption of an N -mer including one internal EMI vibration but ignoring disorder. Then, in Sec. IV, vibrations are ignored but diagonal disorder is considered. In Sec. V, we consider the general case, where an arbitrary number of vibrational normal modes are included and diagonal disorder is present.

We will consider the most simple case when the aggregate is a one-dimensional chain where all the transition dipoles of the monomers are parallel and have the same magnitude. We further restrict to periodic boundary conditions and take only nearest-neighbor interactions into account.

III. ABSORPTION LINE SHAPE IN THE VIBRATIONAL MODEL

We consider first the monomer. Assuming that the electronic transition dipole moment $\langle\phi^e|\boldsymbol{\mu}|\phi^g\rangle$ can be taken as its value at fixed equilibrium Q (Condon approximation), the amplitude a_{eg} for a transition from the vibrational ground state ($\alpha=0$) of the electronic ground state to a vibrational state β of the excited state is given by,

$$a_{eg} \propto \langle\xi^\beta|\langle\phi^e|\boldsymbol{\mu}|\phi^g\rangle|\chi^0\rangle \equiv \boldsymbol{\mu}_{eg}\langle\xi^\beta|\chi^0\rangle. \quad (13)$$

In the harmonic approximation of Eqs. (3) and (6), the overlap integrals $\langle\xi^\beta|\chi^0\rangle$ appearing in Eq. (13) are easily evaluated to give the well-known result³⁸ for the Franck-Condon (FC) factors

$$|f^\beta|^2 \equiv |\langle\xi^\beta|\chi^0\rangle|^2 = \mathfrak{P}_\beta(X), \quad (14)$$

where $X = Q_*^2 \omega / 2\hbar$ is the Huang-Rhys factor³⁸ and $\mathfrak{P}_\beta(X)$ is a discrete Poissonian distribution defined by

$$\mathfrak{P}_\beta(X) = \frac{X^\beta}{\beta!} e^{-X}. \quad (15)$$

Note that the Huang-Rhys factor X completely determines the shape of the Poissonian, in particular, the standard deviation of the Poissonian $\mathfrak{P}_\beta(X)$ is given by \sqrt{X} . With Eq. (14), it follows that the absorption stick spectrum of the monomer is also of Poissonian form i.e.,

$$\mathcal{A}_M(\Omega) \propto \sum_{\beta=0}^{\infty} \mathfrak{P}_\beta(X) \delta(\beta\hbar\omega + \mathcal{E} - \hbar\Omega), \quad (16)$$

where Ω is the frequency of the light. In Eq. (16), constant terms have been omitted, since here we confine interest to the line shape of absorption spectra. Since the “sticks” of the absorption spectrum Eq. (16) have equidistant spacing $\hbar\omega$, it follows that the width (standard deviation) of the monomer absorption spectrum is given by $\sqrt{X}\hbar\omega$.

For strong coupling, as shown by Merrifield³³ and Fulton and Gouterman,¹⁸ the dimer spectrum is also of Poissonian form but with a width reduced by a factor of $\sqrt{2}$ and shifted by the interaction energy V with respect to the monomer spectrum, i.e.,

$$\mathcal{A}_D(\Omega) \propto \sum_{\beta=0}^{\infty} \mathfrak{P}_\beta\left(\frac{X}{2}\right) \delta(\beta\hbar\omega + \mathcal{E} + V - \hbar\Omega). \quad (17)$$

Note that the energy spacing between the absorption peaks remains the same as for the monomer. The narrowing is solely due to the replacement of X by $X/2$.

This behavior is readily explained. As shown by Witkowski and Moffitt,³² in the harmonic approximation, the dimer Hamiltonian is separable, one part corresponding to the symmetric normal coordinate $(Q_1 + Q_2)/\sqrt{2}$ and one part to the asymmetric coordinate $(Q_1 - Q_2)/\sqrt{2}$. The “center-of-mass” symmetric Hamiltonian is independent of V and has eigenstates which are harmonic vibrations giving a Poissonian absorption as in Eq. (17). The asymmetric vibration is coupled to the electronic motion via the interaction V and the Hamiltonian is exactly the Jaynes-Cummings Hamiltonian which appears in the coupling of a harmonic radiation field

to a two-level atom.³⁶ In the strong-coupling limit, the absorption spectrum belonging to this Hamiltonian has only a single line (for parallel transition dipole moments of the monomers). The convolution of this δ function with the Poissonian form of the symmetric vibration gives the spectrum of Eq. (17), as shown in detail in Ref. 36.

Now, this dimer result will be generalized to an N -aggregate of monomers interacting electronically. Again, we will show that the fully symmetric vibration can be separated. Then, as we will see, the only change in the strong-coupling limit is that $(X/2)$ in Eq. (17) for the dimer becomes (X/N) for the aggregate.

In the case of an aggregate, we seek to separate further the total Hamiltonian $\mathcal{H} = \mathcal{H}^s + \mathcal{H}^e$ of Eqs. (10) and (11) by a suitable transformation of the nuclear coordinates,

$$Q'_j = \sum_n Q_n A_{nj}, \quad (18)$$

where A_{nj} are the elements of an orthogonal $N \times N$ transformation matrix A . Defining the momenta P'_j in the same manner, the canonical commutation relations between P'_j and Q'_j still hold and the form of \mathcal{H}^s is unchanged, i.e.,

$$\mathcal{H}^s = \left(\sum_{n=1}^N H_n^s(Q'_n) \right) |g\rangle\langle g| \quad (19)$$

is still a sum of N noninteracting harmonic vibrational Hamiltonians. Noting that the electronic interaction V_{nm} and the transition energy \mathcal{E}_n do not depend on the Q_i , the Hamiltonian operator (12) for the excited electronic states in the new coordinates Q'_j is given by

$$\mathcal{H}^e = \sum_{n=1}^N \left\{ \mathcal{E}_n + \sum_{j=1}^N \frac{1}{2} (P'_j{}^2 + \omega^2 (Q'_j - A_{nj} Q_n)^2) \right\} |\pi_n\rangle\langle \pi_n| + \sum_{nm} V_{nm} |\pi_n\rangle\langle \pi_m|. \quad (20)$$

Choosing $A_{nN} = 1/\sqrt{N}$ for all n and defining the fully symmetric coordinate

$$Q_S = Q'_N = \frac{1}{\sqrt{N}} \sum_n Q_n, \quad (21)$$

the Hamiltonian \mathcal{H}^e can be separated as the sum of two commuting operators,

$$\mathcal{H}^e = \mathcal{H}_S^e + \mathcal{H}_G^e. \quad (22)$$

The part involving the fully symmetric vibration is

$$\mathcal{H}_S^e = \frac{1}{2} \left(P_S^2 + \omega^2 \left(Q_S - \frac{Q^*}{\sqrt{N}} \right)^2 \right) \sum_{n=1}^N |\pi_n\rangle\langle \pi_n|, \quad (23)$$

and the ‘‘generalized’’ Jaynes-Cummings (JC) Hamiltonian is

$$\mathcal{H}_G^e = \sum_{n=1}^N \left\{ \mathcal{E}_n + \sum_{j=1}^{N-1} \frac{1}{2} (P'_j{}^2 + \omega^2 (Q'_j - A_{nj} Q_n)^2) \right\} |\pi_n\rangle\langle \pi_n| + \sum_{nm} V_{nm} |\pi_n\rangle\langle \pi_m|. \quad (24)$$

Irrespective of the geometry of the aggregate, this separation

is always possible as long as the BO potentials are harmonic and identical for all monomers. Note that \mathcal{H}_S^e is completely independent of the electronic exchange coupling and involves a displaced harmonic oscillator in Q_S , whose minimum Q_S^{\min} is shifted by a factor of $1/\sqrt{N}$ less than in the monomer [see Eq. (6)]. The Hamiltonian \mathcal{H}_G^e , however, contains the electronic coupling and the vibronic coupling. We call it the generalized JC Hamiltonian since it was shown³⁶ that for the dimer ($N=2$), the operator \mathcal{H}_G^e is exactly the JC Hamiltonian of quantum optics, describing two electronic levels coupled to oscillatory modes of the electromagnetic field. In the general case of Eq. (24), a total of N electronic states are coupled to the $(N-1)$ oscillatory modes of the nuclear vibrations. The quantity $A_{nj} Q_n^*$ describes a shift of a PES of the collective vibrational coordinate Q'_j upon a local electronic excitation of monomer n . Denoting by $Q_A = \{Q'_i\}$ with $i=1, \dots, N-1$ the set of nuclear coordinates appearing in Eq. (24), the ground electronic state Hamiltonian (19) is simply

$$\mathcal{H}^s = (H^s(Q_S) + H^s(Q_A)) |g\rangle\langle g|. \quad (25)$$

Then, the complete aggregate ground state is

$$|\Psi^s\rangle = |\chi^0(Q_S)\rangle |\chi^0(Q_A)\rangle |g\rangle, \quad (26)$$

and the excited states are

$$|\Psi_l^\beta\rangle = |\xi^\beta(Q_S)\rangle |\Psi_{G,l}(Q_A)\rangle. \quad (27)$$

Here, $|\Psi_{G,l}(Q_A)\rangle$ is the l th eigenstate of the generalized JC Hamiltonian \mathcal{H}_G^e with eigenenergy $E_{G,l}$. Since vibrations and electronic excitation are coupled in Eq. (27), the index l denotes the progression of *vibronic* eigenstates of the operator \mathcal{H}_G^e , which generally have to be determined numerically. Then, from Eqs. (25)–(27), one sees that when one takes the electronic dipole matrix elements $\langle \pi_n | \boldsymbol{\mu} | g \rangle$ at fixed Q 's, the absorption amplitude separates into two factors

$$a_{eg} \propto \langle \xi^\beta(Q_S) | \langle \Psi_{G,l}(Q_A) | \sum_n \boldsymbol{\mu}_n | g \rangle | \chi^0(Q_A) \rangle | \chi^0(Q_S) \rangle = 2 \boldsymbol{\mu}_{eg} \langle \xi^\beta(Q_S) | \chi^0(Q_S) \rangle \langle \xi_{G,l}(Q_A) | \chi^0(Q_A) \rangle, \quad (28)$$

where

$$\langle \xi_{G,l}(Q_A) | = \frac{1}{\sqrt{N}} \langle \Psi_{G,l}(Q_A) | \sum_n | \pi_n \rangle, \quad (29)$$

i.e., the integration has been performed over electronic degrees of freedom but $\xi_{G,l}(Q_A)$ is still a function of the transformed vibrational coordinate. The cross section for absorption is then

$$\mathcal{A}_{\text{agg}}(\Omega) \propto \sum_{\beta=0}^{\infty} \sum_{l=0}^{\infty} |f_S^\beta|^2 |F^l|^2 \delta(\beta \hbar \omega + E_{G,l} - \hbar \Omega), \quad (30)$$

where the FC factors now are defined by

$$|f_S^\beta|^2 = |\langle \xi^\beta(Q_S) | \chi^0(Q_S) \rangle|^2 = \mathfrak{P}_\beta(X/N) = \frac{(X/N)^\beta}{\beta!} e^{-X/N} \quad (31)$$

for the symmetric vibration and

$$|F^l|^2 = |\langle \xi_{G,l}(Q_A) | \chi^0(Q_A) \rangle|^2 \quad (32)$$

involving an integration over the remaining $N-1$ vibrational coordinates $\{Q_i\}$, $i=1, \dots, N-1$. Since, from Eq. (23), the excited symmetric vibration is a displaced harmonic oscillator with displacement Q_*/\sqrt{N} , the $|f_S^\beta|^2$ in Eq. (31) follow a Poisson distribution [Eq. (15)] but with a Huang-Rhys factor $X_S = X/N$, i.e., the width is reduced by a factor of \sqrt{N} with respect to the monomer. Thus, the fully symmetric vibration always separates to provide a Poissonian distribution of FC factors with a width which is the monomer width divided by $1/\sqrt{N}$. Note that the narrowing of this Poissonian distribution stems solely from the reduction of the effective displacement Q_*/\sqrt{N} , since the vibrational quantum of the symmetric vibration does not change compared to that of the monomer.

From Eq. (30), one sees that the aggregate absorption spectrum is a convolution of the Poissonian $a(E) \equiv \sum_{\beta=0}^{\infty} \mathfrak{P}_{\beta}(X/N) \delta(\beta\hbar\omega - E)$ belonging to the symmetric coordinate and the “spectrum” $b(\hbar\Omega) \equiv \sum_l |F^l|^2 \delta(E_{G,l} - \hbar\Omega)$ of the generalized JC Hamiltonian. The question now is what effect do the FC factors $|F^l|^2$ and energies $E_{G,l}$ have on the overall spectral line shape. For the case of a dimer, this has been studied extensively.^{18,36} It was shown that for weak and intermediate couplings the spectrum of the (generalized) JC Hamiltonian consist of many peaks distributed over an energy range of the order of the width of the monomer absorption spectrum. After convolution with the Poisson progression of the symmetric mode, the resulting dimer spectrum has at least a width determined by that of the “JC spectrum.” However, for strong coupling, the JC spectrum consists only of one dominant absorption peak. This peak is shifted by the energy V with respect to the mean of the monomer absorption spectrum. Hence, the dimer absorption spectrum in strong coupling is just the Poissonian progression of the symmetric mode centered at the position of the dominant peak of the JC spectrum. Using the same line of argumentation as was done by Witkowski,³⁴ this strong coupling result can readily be generalized to the case of an N -mer. One then finds for the absorptions spectrum in the limit $2V \gg \sqrt{X}\hbar\omega$

$$A_{\text{agg}}(\Omega) \propto \sum_{\beta=0}^{\infty} \mathfrak{P}_{\beta}(X/N) \delta(\beta\hbar\omega + \tilde{\mathcal{E}} + 2V - \hbar\Omega), \quad (33)$$

with $\tilde{\mathcal{E}} = \mathcal{E} + [(N-1)/N]\sqrt{X}\hbar\omega$. An example of the spectrum given by Eq. (33) is shown in Figs. 2(a)–2(e) (left column) for $X=1$. Since only the change of shape is of interest, to facilitate comparison, the shift $2V$ with respect to the mean energy of the monomer absorption is ignored, i.e., all spectra are centered at their respective mean energies. Figure 2(a) shows the monomer spectrum and Figs. 2(b)–2(e) demonstrate the change of shape of the Poissonian progression. Rapidly the spectrum becomes more and more asymmetric, and the lowest peak gains absorption strength such that already for $N=10$, it carries nearly all the oscillator strength [Fig. 2(d)]. In the right column of Fig. 2, the case of $X=9$ is shown where the monomer line shape is nearly Gaussian. Here, for small N [$N=2$ in Fig. 2(g) and $N=4$ in Fig. 2(h)], the line shape is still approximately Gaussian. For $N=10$ [Fig. 2(i)] again, the spectrum is very asymmetric, and the

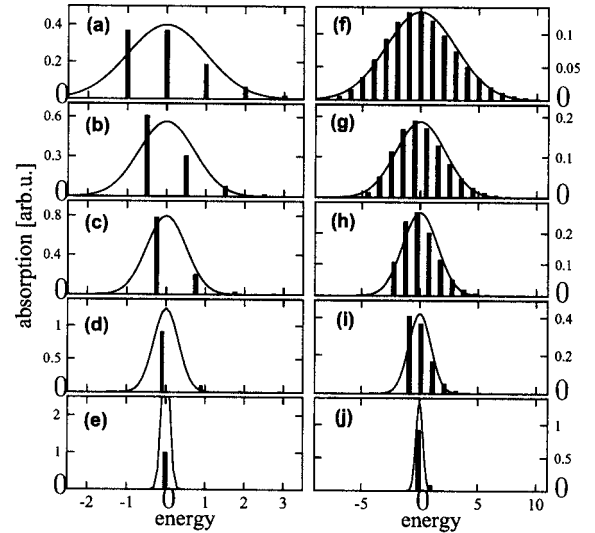


FIG. 2. Strong-coupling absorption spectrum of the symmetric mode with Huang-Rhys factor $X=1$ (left column) and $X=9$ (right column) for increasing N . [(a) and (f)] monomer, [(b) and (g)] dimer, [(c) and (h)] $N=4$, [(d) and (i)] $N=10$, and [(e) and (j)] $N=100$. All spectra are centered about zero and the energy is in units of $\hbar\omega$ of the monomer. For comparison, a continuous Gaussian spectrum with the same variance is shown as a solid line.

lowest peak has dominant absorption strength. For $N=100$, the spectrum is dominated by one peak.

IV. ABSORPTION LINE SHAPE IN THE STATISTICAL MODEL

Here, we consider the relation between the widths of the monomer and aggregate spectra when one ignores vibrations altogether but includes diagonal disorder. Then, the Hamiltonian [Eq. (12)] simplifies considerably. Taking the ground vibrational state of the ground electronic state as the initial state, \mathcal{H}^g , of Eq. (10) merely sets the zero of energy. Then, the Hamiltonian [Eq. (11)] becomes, in nearest-neighbor approximation, simply

$$\mathcal{H}^e = \sum_{n=1}^N \mathcal{E}_n |\pi_n\rangle \langle \pi_n| + \sum_{nm} V_{nm} |\pi_n\rangle \langle \pi_m|. \quad (34)$$

In this diagonal disorder model, the spectral width is assumed to arise from the change of interaction of the monomer with the environment according to its location. It is assumed that the transition energy \mathcal{E}_n of monomer n is distributed according to the probability density $p_n(\mathcal{E}_n)$. Averaging over many (infinite) realizations of the monomer transition energies gives the absorption spectrum. In the case of noninteracting monomers, the absorption line shape is therefore just given by the assumed distribution of transition energies $p_n(\mathcal{E}_n)$.

To investigate the narrowing of the spectrum for strong intermonomer coupling, we will not consider the line shape in detail but focus only on the mean position and the width of the J band. In the following, we will denote the expectation value of a random variable y by $E(y)$ and the variance by $\text{Var}(y)$. To keep the discussion transparent, we take the mean

$$\mathcal{E}_M \equiv E(\mathcal{E}_n) \quad (35)$$

and the variance

$$\sigma_M^2 \equiv \text{Var}(\mathcal{E}_n) \quad (36)$$

of the transition energies \mathcal{E}_n to be the same for all monomers. For one realization of the diagonal disorder of the N -mer, the mean transition energy is given by

$$\bar{\mathcal{E}} = \frac{1}{N} \sum_{n=1}^N \mathcal{E}_n \quad (37)$$

(which is, in general, not equal to the mean transition energy of the monomers \mathcal{E}_M).

In strong coupling ($2V \gg \sigma_M$), we divide the Hamiltonian [Eq. (34)] according to $\mathcal{H}^e = \tilde{H} + W$, where the operator $W \equiv \sum_{n=1}^N (\bar{\mathcal{E}} - \mathcal{E}_n) |\pi_n\rangle \langle \pi_n|$ is a small perturbation to $\tilde{H} \equiv \bar{\mathcal{E}} + \sum_{nm} V_{nm} |\pi_n\rangle \langle \pi_m|$. Using perturbation theory, it was shown in Ref. 19 that in strong coupling, there is only absorption at the energy $\mathcal{E}_{\text{agg}} \equiv \bar{\mathcal{E}} + 2V$. The criterion for the validity of perturbation theory is analyzed also in Ref. 39.

To obtain the mean position $E(\mathcal{E}_{\text{agg}})$ and width (standard deviation σ_{agg}) of the ensemble averaged N -mer absorption spectrum, one needs to calculate the mean and width of the random variable \mathcal{E}_{agg} , which can be done using elementary statistical properties (see, e.g., Ref. 40). One finds for the mean of the aggregate absorption spectrum

$$E(\mathcal{E}_{\text{agg}}) = E(\bar{\mathcal{E}}) + 2V = \mathcal{E}_M + 2V, \quad (38)$$

and for the variance,

$$\sigma_{\text{agg}}^2 \equiv \text{Var}(\mathcal{E}_{\text{agg}}) = \frac{\sigma_M^2}{N} + \frac{2}{N^2} \sum_{n=1}^N \sum_{m<n}^N \text{Cov}(\mathcal{E}_n, \mathcal{E}_m). \quad (39)$$

In the last equation, $\text{Cov}(\mathcal{E}_n, \mathcal{E}_m) = E((\mathcal{E}_n - E(\mathcal{E}_n))(\mathcal{E}_m - E(\mathcal{E}_m)))$ is the covariance of \mathcal{E}_n and \mathcal{E}_m . In deriving Eq. (39), we have used that $\text{Var}(\mathcal{E}_{\text{agg}}) = \text{Var}(\bar{\mathcal{E}})$ and $(1/N^2) \sum_{n=1}^N \text{Var}(\mathcal{E}_n) = \sigma_M^2/N$. To demonstrate the usefulness of Eq. (39), in Appendix A, it is applied to some often used forms of correlation.

For independent transition energies \mathcal{E}_n , the variance of the aggregate absorption spectrum reduces to

$$\sigma_{\text{agg}}^2 = \frac{\sigma_M^2}{N}. \quad (40)$$

Equation (40) shows that the width of the aggregate absorption peak is decreased by $1/\sqrt{N}$ with respect to that of the monomer. The above argument can be generalized straightforwardly to the case where each random variable \mathcal{E}_n has a different mean and different variance. Note that in the derivation of Eqs. (39) and (40), no particular distribution of the transition energies of the monomers has been assumed, showing that the narrowing of the J band occurs irrespective of the monomer line shape (provided the variance is finite), thus generalizing the result obtained for a Gaussian distribution of monomer transition energies. The case of a Gaussian distribution of monomer transition energies is special, since the sum of two Gaussian random variables is again a Gauss-

ian random variable, i.e., the Gaussian is a stable distribution. Furthermore, if the monomer distribution has a finite variance and the correlation between the monomers decreases sufficiently fast with increasing distance between the monomers, then the distribution of \mathcal{E}_{agg} will approach a Gaussian (for more precise requirements of this central limit theorem, see, e.g., Ref. 41). The speed of convergence, i.e., how many monomers N are needed to “approach” a Gaussian distribution, is, in general, quite fast for independent random variables. Examples are discussed in Ref. 40.

The above argument that a narrowing by $1/\sqrt{N}$ occurs [see Eq. (40)] only holds if the variance exists, i.e., $\text{Var}(\mathcal{E}_n) < \infty$. For a Lorentzian (where the second moment does not exist), it was shown numerically in Ref. 13 that no narrowing occurs, irrespective of N and the coupling strength V . For the case of strong coupling, this result is given analytically in Appendix B 1.

A. Poissonian disorder

To compare the disorder model with the vibrational model without disorder, we will investigate the special case when the random variables \mathcal{E}_n are distributed according to a discrete Poisson distribution [Eq. (16)], i.e.,

$$p(\mathcal{E}_n) = \sum_{\beta=0}^{\infty} \mathfrak{P}_{\beta}(X) \delta(\beta\varepsilon + \mathcal{E} - \mathcal{E}_n). \quad (41)$$

This distribution gives exactly the same monomer absorption spectrum as in the purely vibrational model including one IM1 mode with Huang-Rhys factor X and vibrational quantum $\hbar\omega = \varepsilon$. A comparison of the strong-coupling result in the disorder model with the vibrational model is instructive, since it shows the different origin of the narrowing in the two models. As shown in Appendix B in strong coupling in the disorder model, the aggregate line shape can be calculated analytically to give

$$\mathcal{A}_{\text{agg}}(\Omega) \propto \sum_{j=0}^{\infty} \mathfrak{P}_j(NX) \delta\left(j\frac{\varepsilon}{N} + \mathcal{E} - \hbar\Omega\right). \quad (42)$$

Here, again, a Poisson distribution is obtained. However, now, the narrowing stems from the fact that the distance between neighboring peaks is decreased by a factor N , as can be seen in the argument of the delta function. However, the distribution $\mathfrak{P}_j(NX)$, which is responsible for the shape of the spectrum, alone would lead to a width which is \sqrt{N} times that of the monomer. The product of these two effects gives the overall $1/\sqrt{N}$ narrowing. In Figs. 3(a)–3(e), the resulting line shape for increasing length N of the aggregate is shown for a Poissonian with $X=1$. This has to be compared with the results obtained in the vibrational model displayed in the left column of Fig. 2. One clearly sees that in the statistical model with a Poissonian distribution of monomer energies, the aggregate line shape already for $N>4$ becomes Gaussian. This is in contrast to Fig. 2 where the absorption spectrum is dominated by one single peak for $N \geq 4$. This shows the fundamental difference between the vibrational model and the diagonal disorder model. Whereas in the former, the narrowing is accompanied by an increasing asymmetry, in

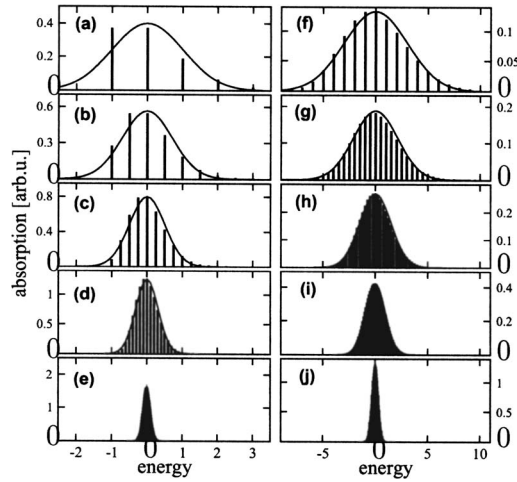


FIG. 3. Strong-coupling absorption line shapes in the statistical model with a distribution function giving a Poissonian line shape with $X=1$ (left column) and $X=9$ (right column) for increasing N . The spectra are calculated using Eq. (42). [(a) and (f)] monomer, [(b) and (g)]: Dimer, [(c) and (h)] 4-mer, [(d) and (i)] 10-mer, [(e) and (j)] 100-mer. All spectra are centered about zero and the energy is in units of $\hbar\omega$ of the monomer. These spectra are to be compared to those shown in Fig. 2.

the latter, the spectrum rapidly assumes a symmetric Gaussian line shape as N increases.

V. BOTH VIBRATIONS AND DISORDER

In the previous sections, we have investigated two different models which describe how the J band narrows with increasing number N of monomers forming the aggregate. One model assumes that each monomer possesses a single vibrational mode. In this model, all monomers in the aggregate have identical properties, whereas in the statistical model of Sec. IV, vibrations are ignored but it is assumed that the transition energies of the monomers are randomly distributed. It was shown that in both cases, the width of the J band is decreased by a factor of $1/\sqrt{N}$ with respect to the width of the monomer. We will now discuss how these models can be merged and extended.

In the following, we will consider ν_{\max} vibrational modes of type IM1 for one monomer. These modes are assumed to be normal modes. The respective coordinate belonging to mode ν is denoted by $Q_{(\nu)}$. The frequencies, the shifts of the upper harmonic potential curves, and the Huang-Rhys factors of these normal modes are denoted by $\omega_{(\nu)}$, $Q_{*_{(\nu)}}$, and $X_{(\nu)}$, respectively. The FC factor for a transition from the ground vibrational state of the electronic ground state to the β th state in the electronic excited state of normal mode ν is

$$|f_{(\nu)}^{\beta}|^2 = \mathfrak{R}_{\beta}(X_{(\nu)}) = \frac{X_{(\nu)}^{\beta}}{\beta!} e^{-X_{(\nu)}}. \quad (43)$$

Furthermore, diagonal disorder is taken into account where the electronic transition energies of the monomers are distributed with a distribution function p , which, for simplicity, is chosen identical for all monomers. The absorption spectrum of the noninteracting monomers can then be written as

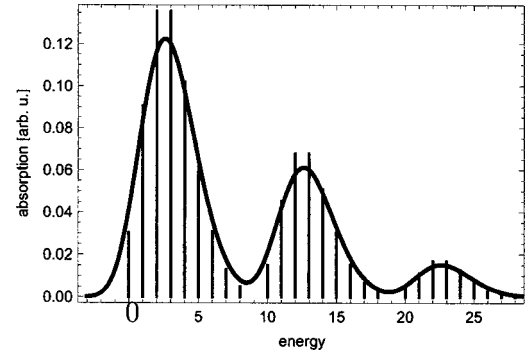


FIG. 4. Monomer spectrum calculated with Eq. (44) using two IM1 normal modes (sticks) and an additional Gaussian disorder (solid line). The energy is in units of $\hbar\omega_{(2)}$. The parameters used for the IM1 modes are $X_{(1)}=0.5$, $X_{(2)}=3$, $\omega_{(1)}=10\omega_{(2)}$, and the width of the Gaussian distribution is $\sigma_{\text{dis}}=1$.

$$\mathcal{A}_M(\Omega) \propto \sum_{\beta_1, \dots, \beta_{\nu_{\max}}} |f_{(1)}^{\beta_1}|^2 \dots |f_{(\nu_{\max})}^{\beta_{\nu_{\max}}}|^2 \times p\left(\sum_{\nu} \beta_{\nu} \hbar \omega_{(\nu)} + \mathcal{E} - \hbar \Omega\right). \quad (44)$$

An example of such a spectrum is shown in Fig. 4. Denoting by σ_{dis} the width of the diagonal disorder distribution, the width Δ of the monomer spectrum is

$$\Delta = \sqrt{\sigma_{\text{dis}}^2 + \sum_{\nu} X_{(\nu)} (\hbar \omega)^2}. \quad (45)$$

Now, consider the aggregate. Applying the transformation A [see Eqs. (18) and (21)] to each coordinate $Q_{(\nu)}$ allows a separation $\mathcal{H}^e = \mathcal{H}_S^e + \mathcal{H}_G^e$ [see Eq. (22)], where

$$\mathcal{H}_S^e = \sum_{\nu} \frac{P_{S(\nu)}^2}{2} + \frac{\omega_{(\nu)}^2}{2} \left(Q_{S(\nu)} - \frac{Q_{*_{(\nu)}}}{\sqrt{N}} \right)^2 \quad (46)$$

is just a sum of shifted harmonic oscillators for each normal mode and

$$\mathcal{H}_G^e = \sum_{n=1}^N \left\{ \mathcal{E}_n + \sum_{j=1}^{N-1} \sum_{(\nu)} \frac{1}{2} (P_{j(\nu)}'^2 + \omega_{(\nu)}^2 (Q_{j(\nu)}' - A_{nj} Q_{*_{(\nu)}})^2) \right\} \times |\pi_n\rangle \langle \pi_n| + \sum_{nm} V_{nm} |\pi_n\rangle \langle \pi_m|. \quad (47)$$

Equation (30) can now be generalized directly to more than one vibrational mode, and one obtains for the aggregate absorption spectrum

$$\mathcal{A}_{\text{agg}}(\Omega) \propto \sum_{\beta_1, \dots, \beta_{\nu_{\max}}} |f_{S(1)}^{\beta_1}|^2 \dots |f_{S(\nu_{\max})}^{\beta_{\nu_{\max}}}|^2 \times \sum_l \left\langle \left\langle |F^l|^2 \delta\left(\sum_{\nu} \beta_{\nu} \hbar \omega_{(\nu)} + E_{G,l} - \hbar \Omega\right) \right\rangle \right\rangle, \quad (48)$$

with FC factors of the symmetric mode given by

$$|F_{S(v)}^\beta|^2 = \mathfrak{P}_\beta \left(\frac{X(v)}{N} \right) \quad (49)$$

and $\langle\langle \dots \rangle\rangle$ denotes the average over disorder. Note that the FC factors $|F|^2$ and eigenenergies $E_{G,l}$ of the generalized JC part are now dependent on the particular realization of the transition energies \mathcal{E}_n . Note also that Eq. (48) is equivalent to a convolution of Poissonians $a_{(v)}(E) = \sum_{\beta_v} \mathfrak{P}_{\beta_v} (X(v)/N) \delta(E - \beta_v \hbar \omega_{(v)})$ with the spectrum of the generalized JC part $b(E) = \langle\langle \sum_l |F|^2 \delta(E - E_{G,l}) \rangle\rangle$, i.e., $\mathcal{A}_{\text{agg}} = b * a_1 * \dots * a_{v_{\text{Max}}}$, where $*$ denotes the convolution.

Using arguments similar to those of Secs. III and IV, one sees that in strong coupling ($2V \gg \Delta$), the FC factor $|F^0|^2$ which belongs to the transition with energy $E_{G,0} = \bar{\mathcal{E}} + 2V + [(N-1)/N] \sum_v \sqrt{X(v)} \hbar \omega_{(v)}$ carries all the oscillator strength, where $\bar{\mathcal{E}}$ is given by Eq. (37). As in Sec. IV, the width of the distribution of $E_{G,0}$ is given by the width of the distribution of $\bar{\mathcal{E}}$. According to Eq. (40), this distribution has narrowed by a factor of \sqrt{N} with respect to the monomer disorder distribution. Also, since the width of the Poissonian progressions $a_{(v)}(E)$ of the normal modes has narrowed by a factor of \sqrt{N} , the absorption spectrum of the N -mer has also narrowed by a factor of \sqrt{N} , which can easily be seen using the properties of the convolution of these distributions.

For the special case that the disorder is Gaussian (with variance σ_{dis}^2 and mean \mathcal{E}_M), one obtains for the absorption spectrum of the aggregate in strong coupling

$$\mathcal{A}_{\text{agg}}(\Omega) \propto \sum_{\beta_1, \dots, \beta_{v_{\text{max}}}} \mathfrak{P}_{\beta_1} \left(\frac{X_1}{N} \right) \dots \mathfrak{P}_{\beta_{v_{\text{max}}}} \left(\frac{X_{v_{\text{max}}}}{N} \right) \times G \left(\sum_v \beta_v \hbar \omega_{(v)} + \bar{\mathcal{E}} + 2V - \hbar \Omega \right), \quad (50)$$

where G is again a Gaussian distribution but with variance σ_{dis}^2/N and $\bar{\mathcal{E}} = \mathcal{E}_M + [(N-1)/N] \sum_v \sqrt{X_v} \hbar \omega_{(v)}$.

We have performed numerical diagonalizations of the Hamiltonian [Eq. (12)] and have compared the resulting “exact” spectra with the analytic expression for strong coupling [Eq. (50)]. This comparison is shown in Fig. 5 for $N=2$ and $N=4$ and considering one vibrational mode with $X=0.49$ and Gaussian disorder with a standard deviation $0.5\hbar\omega$. Figure 5(a) shows the monomer spectrum. The unit of energy is the vibrational quantum $\hbar\omega$ and the zero of energy is at the mean energy of the absorption spectrum. Due to the disorder, the vibrational progression of the monomer is broadened into a single peak, although the asymmetry of the monomer spectrum is still evident. Figures 5(b) and 5(c) show the case $N=2$ and $N=4$ calculated in the strong-coupling limit. For all spectra, the results (dotted lines) using Eq. (50) agree very well with the numerical calculations (solid lines). Due to the narrowing of the Gaussian disorder distribution, already in the case of the dimer, the vibrational progression of the symmetric mode becomes visible. In the case of the 4-mer, the vibrational peaks are clearly resolved.

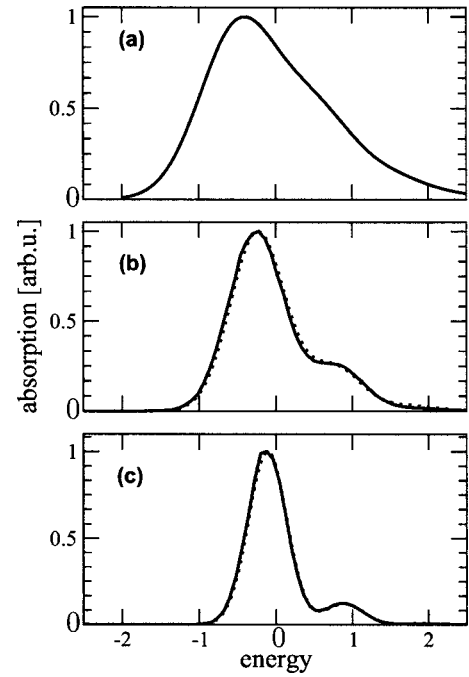


FIG. 5. Comparison between the aggregate spectrum calculated according to Eq. (50) (dotted line) and numerical diagonalization of the aggregate Hamiltonian (solid). (a) monomer, (b) dimer, and (c) $N=4$. All spectra calculated with Huang-Rhys factor $X=0.49$ and Gaussian disorder with a standard deviation of $0.5\hbar\omega$.

VI. DISCUSSION

We have examined the width of the J band in the limit of extremely strong-excitonic coupling predicted by various theories. In a model of identical monomers but including intramolecular vibrations, we have shown that the fully symmetric vibration of the N -monomer aggregate can be separated. A Poisson line shape for the monomer vibronic levels gives rise to an aggregate Poisson line shape with the same vibrational spacing but of width reduced by $1/\sqrt{N}$. This spectrum folded with the single absorption line due to a 0–0 transition in the remaining coordinates gives the absorption spectrum of the aggregate in the strong-coupling limit. This analysis is a straightforward generalization of the old and well-known analysis of the dimer by Merrifield.³³

A model of spectral shapes very common in the literature is one in which vibrations are ignored altogether but the “site energies,” i.e., the electronic transition energy of each of the N monomers are assumed to be distributed statistically. For a Gaussian, the most common assumed distribution, it has been shown long ago that exchange narrowing leads (for uncorrelated site energies) to a $1/\sqrt{N}$ reduction of the J -band width compared to the assumed width. Here, the same result has been shown to hold quite generally, irrespective of the chosen distribution of site energies, provided it has a finite variance. Then, for large N , the line shape of the J band will also assume a Gaussian line shape due to the central limit theorem. In Appendix A, the method is extended to treat the case of correlated site energies. It has also been demonstrated (see Appendix B 1) that for a Lorentz distribution, which has no finite variance, no narrowing occurs, even for uncorrelated disorder.

Considering the case of a discrete Poisson distribution, which gives the same absorption line shape as in the vibrational model, the origin of the $1/\sqrt{N}$ factor has been traced to the fact that, unlike in the vibrational case, the Poisson distribution broadens by a factor of \sqrt{N} (and becomes more and more Gaussian) but simultaneously the vibrational spacing decreases by a factor of $1/N$.

We have derived the strong-excitonic coupling absorption spectrum for the combined case of coupling to internal vibrational modes (IM1) and diagonal disorder. This spectrum shows features of both narrowing mechanisms. As can be seen in Figs. 5(b) and 5(c), each individual peak of a vibrational progression narrows as predicted by the statistical model, but also the overall vibrational progression narrows, as in the purely vibrational model. This is seen by imagining the broad peaks in Figs. 5(a)–5(c) to be replaced by sticks at their center. Then, the curves in Fig. 5 are quantitatively similar to those of Figs. 2(a)–2(c). It is also encouraging that the approximate formula [Eq. (50)] gives almost perfect agreement with exact numerical results for $N=2$ and $N=4$. This implies that the formula may be useful in practice.

In all this discussion, one should be aware that the width of an N -aggregate peak is not a well-defined quantity, in that it is local rather than global. Indeed, an exact sum rule, proved for $N=2$ by Fulton and Gouterman¹⁸ and later generalized to all N ,^{42–44} states that the width of the N -mer absorption is *identical* to that of the monomer and certainly not $1/\sqrt{N}$ smaller. The origin of this discrepancy is to be found in a small but finite absorption into other levels, far removed from the J band. The contribution of this absorption to the global width restores the sum rule, as has been shown explicitly for the dimer.^{18,45}

One problem with the above theories, as already mentioned, is to ascertain in an experimental situation quite what is N or the effective N_{coh} . Although Malyshev *et al.*^{27,30,31} have proposed a formula for N_{coh} in the disorder model, certainly this question needs more research. An alternative theory, where the narrowing is independent of N , must be mentioned here. This is the CES approximation which the present authors have applied to calculate the J and H bands of several dye aggregate spectra.^{9–12} The CES approximation satisfies the exact sum rule on the global width.⁴⁴ However, in strong coupling, an approximate expression can be derived for the local width of the J band.¹³ In agreement with the statistical model, a monomer Lorentzian is simply shifted unchanged in shape. For a Gaussian, in the CES approximation, the prediction is a J -band width decreasing exponentially with the square of the energy shift, in apparent contradiction to the $1/\sqrt{N}$ rule. However, the tail of the monomer spectrum, which decides the J -band width in CES approximation, is never truly Gaussian in practice. In realistic cases, i.e., for the Urbach exponential tail, the CES result is in close agreement with experiment.¹²

It is also interesting that the CES approximation gives an expression for the spectral absorption function which is almost identical to that of Klafter and Jortner¹⁵ who assumed a Gaussian distribution of site energies and included model exciton-vibrational coupling. In both theories, the aggregate spectral function for absorption at energy E is proportional to

the imaginary part of the averaged aggregate Green's function $\langle G(E) \rangle$. In CES approximation, this is explicitly

$$-\text{Im}\langle G(E) \rangle = -\text{Im} \frac{\langle g(E) \rangle}{1 - 2V\langle g(E) \rangle}, \quad (51)$$

where $\langle g(E) \rangle$ is the monomer averaged Green's function and $2V$ is the excitonic coupling. Writing the real and imaginary parts of $\langle g(E) \rangle$ as g_R and g_I , respectively, and taking J -band absorption to be centered at $E \approx 2V$ in strong coupling, one has

$$-\text{Im}\langle G(E) \rangle = -\frac{1}{2V} \text{Im} \frac{2Vg_I(E)}{(E - 2V)^2 + (2Vg_I(E))^2}, \quad (52)$$

where we have used a dispersion relation to put $g_R \approx 1/E$ for strong coupling.¹³ This expression is identical in form to Eq. (II.8) of Ref. 15 where the complex self-energy replaces the complex $2V\langle g_I(E) \rangle$.

It is hoped that the above results are certainly of interest to theorists, since they combine two apparently rather different approaches. However, they are only valid in the limit of very large coupling. Unfortunately, most experimental data do not allow a definitive test of these theories, since one encounters coupling strengths of the order of a few Δ , e.g., $\text{SP} \sim 2$ to $\text{SP} \sim 3$, even though a clearly identifiable narrow J band is formed.

ACKNOWLEDGMENTS

Financial support of the DFG in the Project No. Br 728/11 is acknowledged gratefully.

APPENDIX A: EXAMPLES OF CORRELATED DISORDER

To investigate the influence of correlations and the use of Eq. (39), we consider several models which are used in the literature. As a first example, we assume that the spatial correlations between the monomer transition energies decay exponentially with a correlation length a . This assumption leads to¹⁹

$$\text{Cov}(\mathcal{E}_n, \mathcal{E}_m) = \sigma_M^2 e^{-a|n-m|}, \quad \text{linear aggregates}, \quad (A1)$$

$$\begin{aligned} \text{Cov}(\mathcal{E}_n, \mathcal{E}_m) &= \sigma_M^2 \frac{\cosh\left(a\left(\frac{N}{2} - |n-m|\right)\right)}{\cosh\left(a\frac{N}{2}\right)}, \quad \text{cyclic aggregates.} \end{aligned} \quad (A2)$$

Inserting these expressions in Eq. (39) and defining $b = e^{-a}$, one finds for the variance of the aggregate by a simple calculation,

$$\sigma_{\text{agg}}^2 = \frac{\sigma_M^2}{N} \left(1 + \frac{2b}{1-b} + \frac{2b}{N} \frac{b^N - 1}{(1-b)^2} \right), \quad \text{linear aggregates}, \quad (A3)$$

$$\sigma_{\text{agg}}^2 = \frac{\sigma_M^2(1+b)(1-b^N)}{N(1-b)(1+b^N)}, \quad \text{cyclic aggregates.} \quad (\text{A4})$$

These results agrees with those derived by Knapp¹⁹ for a Gaussian distribution. The derivation given here is much simpler and more general, since no specific distribution has been assumed.

As a second example of Eq. (39), we consider a model for correlations which has recently been studied by Malyshev *et al.*⁴⁶ In this model, one assumes that the aggregate consists of S segments, each containing L monomers ($SL = N$). Within each segment, the transition energies \mathcal{E}_n are equal, but the energies of the segments are distributed according to a probability distribution with width σ_M . Thus, one has $\text{Cov}(\mathcal{E}_n, \mathcal{E}_m) = \sigma_M^2$ for n and m within the same segment and $\text{Cov}(\mathcal{E}_n, \mathcal{E}_m) = 0$ otherwise. Now, one has $\sum_{n=1}^N \sum_{m < n}^N \text{Cov}(\mathcal{E}_n, \mathcal{E}_m) = SL(L-1)/2$ and, inserting this into Eq. (39), one finally obtains

$$\sigma_{\text{agg}}^2 = \sigma_M^2 \frac{L}{N}, \quad (\text{A5})$$

which is the result obtained in Ref. 46 for a Gaussian distribution.

APPENDIX B: SPECIAL CASES OF DISORDER

In this appendix, we calculate the line shape of the J band for special cases of the diagonal disorder distribution. The first example is a Lorentzian distribution. This distribution does not have a finite width. As will be demonstrated, the J band has the same Lorentzian line shape, i.e., no narrowing occurs. For the second example, we have chosen a discrete Poissonian distribution to compare with the vibrational monomer line shape. We restrict to independent random variables.

To obtain the J -band line shape (in strong coupling), we have to calculate the distribution $P(\bar{\mathcal{E}})$ of the random variable $\bar{\mathcal{E}} = (1/N) \sum_{n=1}^N \mathcal{E}_n$, see Eq. (37). It is well known (see, e.g., Ref. 40) that the probability density function of the sum of two independent random variables is given by the convolution by their respective probability densities. Denoting by $p_n(\mathcal{E}_n)$ the distribution of the random variable \mathcal{E}_n , we have

$$P(\bar{\mathcal{E}}) = N f_1(N\bar{\mathcal{E}}) = N p_1 * \cdots * p_N(N\bar{\mathcal{E}}), \quad (\text{B1})$$

where $*$ denotes the convolution. Thus, the distribution of the energies $\bar{\mathcal{E}}$ can be obtained by successively convoluting the monomer distributions p_N, \dots, p_1 . We, will now use this result for the cases of a Lorentzian and Poissonian monomer distributions.

1. Lorentzian

It is easy to show that the convolution of two Lorentzians with Γ_1 and Γ_2 is again a Lorentzian, but with width $\Gamma_1 + \Gamma_2$. With this and Eq. (B1), one obtains

$$P(\bar{\mathcal{E}}) = N \frac{1}{\pi} \frac{\sum_{j=1}^N \Gamma_j}{(\bar{\mathcal{E}}N)^2 + (\sum_j \Gamma_j)^2} = \frac{1}{\pi} \frac{\sum_{j=1}^N \Gamma_j}{\bar{\mathcal{E}}^2 + \left(\frac{1}{N} \sum_j \Gamma_j\right)^2}. \quad (\text{B2})$$

For the case of identical Lorentzians of the monomer distributions, i.e., $\Gamma_j = \Gamma$ for all j , one finds that the distribution $P(\bar{\mathcal{E}})$ is identical to that of a single monomer.

Poissonian

To prove Eq. (42), we first consider the convolution of two distributions given by

$$p_n(\mathcal{E}_n) = \sum_{\beta=0}^{\infty} X^\beta \frac{e^{-X}}{\beta!} \delta(\beta\mathcal{E} + \mathcal{E} - \mathcal{E}_n). \quad (\text{B3})$$

The result for the N -mer follows then by repeating the same line of argumentation.

We find for the convolution of p_1 and p_2

$$\begin{aligned} p_1 * p_2(y) &= \int p_1(x) p_2(y-x) dx \\ &= \sum_{\beta_1, \beta_2} \frac{X^{\beta_1 + \beta_2}}{\beta_1! \beta_2!} e^{-2X} \delta(2\mathcal{E} + (\beta_1 + \beta_2)\mathcal{E} - y) \\ &= \sum_{j=0}^{\infty} \frac{(2X)^j e^{-2X}}{j!} \delta(2\mathcal{E} + j\mathcal{E} - y). \end{aligned} \quad (\text{B4})$$

In the last step, $j = \beta_1 + \beta_2$ was introduced and the identity

$$\sum_{\beta_1} \frac{X^j}{\beta_1! (j - \beta_1)!} = \frac{X^j}{j!} \sum_{\beta_1} \binom{j}{\beta_1} = \frac{(2X)^j}{j!} \quad (\text{B5})$$

was used. With Eq. (B1), the result [Eq. (42)] follows directly from Eq. (B4).

¹E. E. Jelley, *Nature* (London) **138**, 1009 (1936).

²G. Scheibe, *Angew. Chem.* **49**, 563 (1936).

³G. Scheibe, *Angew. Chem.* **50**, 212 (1937).

⁴G. Scheibe, *Kolloid-Z.* **82**, 1 (1938).

⁵J. Franck and E. Teller, *J. Chem. Phys.* **6**, 861 (1938).

⁶M. Wewer and F. Stienkemeier, *J. Chem. Phys.* **120**, 1239 (2004).

⁷W. T. Simpson and D. L. Peterson, *J. Chem. Phys.* **26**, 588 (1957).

⁸J. S. Briggs and A. Herzenberg, *Mol. Phys.* **21**, 865 (1971).

⁹A. Eisfeld and J. S. Briggs, *Chem. Phys.* **281**, 61 (2002).

¹⁰A. Eisfeld and J. S. Briggs, *Chem. Phys.* **324**, 376 (2006).

¹¹A. Eisfeld, R. Kniprath, and J. Briggs, *J. Chem. Phys.* **126**, 104904 (2007).

¹²A. Eisfeld and J. S. Briggs, *Chem. Phys. Lett.* **446**, 354 (2007).

¹³A. Eisfeld and J. S. Briggs, *Phys. Rev. Lett.* **96**, 113003 (2006).

¹⁴J. Klafter and J. Jortner, *Chem. Phys. Lett.* **50**, 202 (1977).

¹⁵J. Klafter and J. Jortner, *J. Chem. Phys.* **68**, 1513 (1978).

¹⁶J. Klafter and J. Jortner, *Chem. Phys.* **26**, 421 (1977).

¹⁷A. V. Lukashin and M. D. Frank-Kamenetskiĭ, *Chem. Phys. Lett.* **45**, 36 (1977).

¹⁸R. L. Fulton and M. Gouterman, *J. Chem. Phys.* **41**, 2280 (1964).

¹⁹E. W. Knapp, *Chem. Phys.* **85**, 73 (1984).

²⁰E. W. Knapp, P. O. J. Scherer, and S. F. Fischer, *Chem. Phys. Lett.* **111**, 481 (1984).

²¹D. L. Huber and W. Y. Ching, *Phys. Rev. B* **39**, 8652 (1989).

²²H. Fidler, J. Knoester, and D. A. Wiersma, *J. Chem. Phys.* **95**, 7880 (1991).

²³F. Domínguez-Adame and V. A. Malyshev, *J. Lumin.* **83-4**, 61 (1999).

²⁴C. Didruga and J. Knoester, *Chem. Phys.* **275**, 307 (2002).

²⁵M. Wubs and J. Knoester, *Chem. Phys. Lett.* **284**, 63 (1998).

²⁶A. Tilgner, H. P. Trommsdorff, J. M. Zeigler, and R. M. Hochstrasser, *J.*

- Lumin. **45**, 373 (1990).
- ²⁷ V. A. Malyshev and F. Dominguez-Adame, Chem. Phys. Lett. **313**, 255 (1999).
- ²⁸ M. Bednarz, V. A. Malyshev, and J. Knoester, Phys. Rev. Lett. **91**, 217401 (2003).
- ²⁹ P. Scherer, in *J-Aggregates*, edited by T. Kobayashi (World Scientific, Singapore, 1996).
- ³⁰ V. A. Malyshev, Opt. Spektrosk. **71**, 873 (1991) [Opt. Spectrosc. **71**, 505 (1991)].
- ³¹ V. A. Malyshev, J. Lumin. **55**, 225 (1993).
- ³² A. Witkowski and W. Moffitt, J. Chem. Phys. **33**, 872 (1960).
- ³³ R. E. Merrifield, Radiat. Res. **20**, 154 (1963).
- ³⁴ A. Witkowski, in *Modern Quantum Chemistry III*, edited by O. Sinanoğlu (Academic, New York, 1965), Chap. III 3, pp. 161–175.
- ³⁵ P. O. J. Scherer and S. F. Fischer, Chem. Phys. **86**, 269 (1984).
- ³⁶ A. Eisfeld, L. Braun, W. T. Strunz, J. S. Briggs, J. Beck, and V. Engel, J. Chem. Phys. **122**, 134103 (2005).
- ³⁷ J. Seibt, P. Marquetand, V. Engel, Z. Chen, V. Dehn, and F. Würthner, Chem. Phys. **328**, 354 (2006).
- ³⁸ E. S. Medvedev and V. I. Osherov, *Radiationless Transitions in Polyatomic Molecules*, of Springer Series in Chemical Physics Vol. 57 (Springer-Verlag, Berlin, 1995).
- ³⁹ F. Dominguez-Adame and V. A. Malyshev, Am. J. Phys. **72**, 226 (2004).
- ⁴⁰ A. Papoulis, *Probability, Random-Variables, and Stochastic Processes* (McGraw-Hill, New York, 1991).
- ⁴¹ B. Nahapetian, *Limit Theorems and Some Applications in Statistical Physics* (Teubner, Leipzig, 1991).
- ⁴² J. S. Briggs and A. Herzenberg, Proc. Phys. Soc. London **92**, 159 (1967).
- ⁴³ R. E. Merrifield, J. Chem. Phys. **48**, 3693 (1968).
- ⁴⁴ J. S. Briggs and A. Herzenberg, J. Phys. B **3**, 1663 (1970).
- ⁴⁵ J. S. Briggs and A. Herzenberg, Mol. Phys. **23**, 203 (1972).
- ⁴⁶ V. A. Malyshev, A. Rodriguez, and F. Dominguez-Adame, Phys. Rev. B **60**, 14140 (1999).